1

A Generic Thermal Model for Perfused Tissues

Devashish Shrivastava[1,2*]

[1] *US Food and Drug Administration, Silver Spring, MD, USA*
[2] In Vivo *Temperatures, LLC, Burnsville, MN, USA*

COPYRIGHTED MATERIAL

1.1 Introduction

Many diagnostic and therapeutic procedures require a thermal model for perfused tissues for determining *in vivo* temperatures in order to better plan and implement those procedures (e.g., heating during MRI, burn management, etc.). However, it is extremely challenging to determine *in vivo* temperatures by solving the 'exact' thermal model, derived from first principles, and called the convective energy equation (CEE) [1]. This is so because it requires at least 20 linear computational nodes across the diameter of a blood vessel to obtain a numerically converged temperature solution of the CEE [2]. Blood vessel diameters range from ~3 cm in large vessels (e.g., aorta, vena cava) to ~3 μm in capillaries inside a human body. Thus, it requires a stupendous amount of computational power (~$3(10^{11})$ nodes for every 1 mm^3 assuming a uniform mesh resolution of 0.15 μm) to solve for the temperatures in perfused tissues if the CEE is used alone. This is in addition to the daunting challenge of knowing the blood velocity field in all the vessels down to every single capillary as a function of space and time since the blood velocity is a necessary input to the CEE. Therefore, to manage computational costs, temperatures in tissues embedded with 'small' (<1 mm in diameter) more frequent blood vessels are determined using 'approximate' thermal models known as bioheat transfer models (BHTMs) [3, 4], and temperatures in 'large' (vessel diameter ≥ 1 mm), less frequent blood vessels are determined using the 'exact' thermal model, the CEE [1].

BHTMs can be derived using first principles or proposed intuitively. The objective of this chapter is to present a general methodology to derive BHTMs from first principles. Deriving BHTMs from first principles is important since it helps relate the variables and parameters of the bioheat models to the underlying physiology, which provides better insight into the most fundamental mechanisms at play. The methodology is used to, first, derive a general, 'two-compartment' BHTM with very few assumptions – herein called the two-compartment generic bioheat transfer model (GBHTM) [5]. Later, more general forms of the model (i.e., a three-compartment GBHTM and an '$N + 1$'

* Corresponding author: devashish.shrivastava@gmail.com

Theory and Applications of Heat Transfer in Humans, First Edition. Edited by Devashish Shrivastava.
© 2018 John Wiley & Sons Ltd. Published 2018 by John Wiley & Sons Ltd.

compartment GBHTM) are derived using the same methodology. Next, the newly derived two-compartment GBHTM is compared with Pennes' intuitively proposed (and thus, empirical) 'gold standard' BHTM to better understand the implicit and explicit assumptions, and thereby application regime of Pennes' BHTM. Pennes' BHTM is chosen since it is a simple, empirical, and widely used BHTM. Lack of a formal derivation makes it difficult to relate the parameters and variables of this simple BHTM to the underlying physiology (e.g., blood flow, blood vasculature geometry, thermal properties of tissue and blood vessels), which in turn has, historically, made the implementation and interpretation of Pennes' BHTM and its results controversial and unreliable. Finally, *in vivo* temperature predictions of the two-compartment GBHTM and Pennes' BHTM are compared to the measured temperatures for magnetic resonance imaging (MRI) applications to further illustrate the usefulness of the bioheat models.

1.2 Derivation of Generic Bioheat Thermal Models (GBHTMs)

Above, we discuss the complexity and the impracticality of solving the exact thermal model, the CEE, alone in perfused tissues to obtain point-wise true tissue temperature distribution in space and time. That scenario forces us, as a compromise, to develop an approximate thermal model to determine the temperature of a 'volume' of tissue (i.e., a 'volume averaged' tissue temperature), rather than determining the temperature of each point in tissue (i.e., point-wise true tissue temperature).

Let's derive an approximate thermal model, a two-compartment GBHTM, by volume averaging the CEE. The presented methodology is general and is used to derive a three-compartment GBHTM and an '$N + 1$' compartment GBHTM later in this chapter. For those of you who are not interested in the derivation, you may refer directly to the final differential form of the two-compartment GBHTM presented in Equations 1.10 and 1.11 below. The three-compartment GBHTM is presented in Equations 1.12–1.14. The '$N + 1$' compartment GBHTM is presented in Equations 1.15, 1.16. Simplifications used to obtain the GBHTMs are presented in Equations 1.7–1.9.

1.2.1 A Two-Compartment Generic Bioheat Transfer Model

Let's consider a finite, vascularized, heated tissue. Let's assume that the blood stays inside the vasculature and everything surrounding the blood is a non-moving solid tissue. Conserving energy at a point in the solid tissue and blood results in the following point-wise true, exact thermal model, the CEE [1]. Note that the velocity of solid tissue u_T is zero in Equation 1.1 by our assumption.

$$(\rho c_P)_i \left[\frac{\partial T_i}{\partial t} + u_i.\nabla T_i\right] = \nabla.k_i \nabla T_i + Q_i,\ i = T, Bl \tag{1.1}$$

Also, note that solving Equation 1.1 for the point-wise temperatures in tissue perfused with smaller (<1 mm in diameter), more frequent blood vessels is impractical due to the tremendous cost of computation and the unavailability of the three-dimensional blood velocity field u_{Bl}. Next, let's imagine that our perfused tissue is made of several smaller volumes put together, herein called the averaging volume and each averaging volume V

consists of two sub-volumes or compartments: a solid tissue sub-volume V_T and blood sub-volume V_{Bl}. Integrating Equation 1.1 over the solid tissue and blood sub-volumes, separately, in an averaging volume results in Equation 1.2.

$$\int_{V_i} (\rho c_P)_i \left[\frac{\partial T_i}{\partial t} + u_i.\nabla T_i\right] dV = \int_{V_i} (\nabla.k_i \nabla T_i) dV + \int_{V_i} Q_i dV,\ i = T, Bl \tag{1.2}$$

Applying divergence theorem to the first terms on the left-hand side (LHS) and right-hand side (RHS) of Equation 1.2 results in Equation 1.3. Interested readers are encouraged to derive Equation 1.3 using Equation 1.2 for themselves.

$$\int_{V_i} (\rho c_P)_i \frac{\partial T_i}{\partial t} dV - \int_{V_i} T_i \nabla.(\rho c_P u)_i\, dV = \int_{S_{out-i}} [(-k_i \nabla T_i) - (\rho c_P)_i u_i T_i].n_{out-i}\, dS + \int_{S_{j-i}} (-k_i \nabla T_i).n_{j-i}\, dS + \int_{V_i} Q_i\, dV \tag{1.3}$$

where, i and $j = T, Bl$ and $i \neq j$.

Assuming (a) constant density, (b) constant specific heat, and (c) incompressible blood and blood vessels in the averaging blood sub-volume, the second term on the LHS reduces to zero due to the principle of conservation of mass. (Note that this term is zero for solid tissue since $u_T = 0$.) Thus, Equation 1.3 simplifies as follows.

$$\int_{V_i} (\rho c_P)_i \frac{\partial T_i}{\partial t} dV = \int_{S_{out-i}} [(-k_i \nabla T_i) - (\rho c_P)_i u_i T_i].n_{out-i}\, dS + \int_{S_{j-i}} (-k_i \nabla T_i).n_{j-i}\, dS + \int_{V_i} Q_i\, dV \tag{1.4}$$

where, $i = j = T, Bl$ and $i \neq j$.

In Equation 1.4, the first term on the RHS represents the energy gained by a solid tissue (or blood) sub-volume from adjacent solid tissue (or blood) sub-volumes. The second term on the RHS represents the energy exchange due to the interaction between the solid tissue and blood sub-volumes inside an averaging volume. The third term on the RHS represents the energy gained by the solid tissue (or blood) sub-volume in an averaging volume due to source terms.

Next, normalizing Equation 1.4 by sub-volume V_i the following general integral form of the generic BHTM (Equation 1.5) is obtained. This form satisfies the energy equation and is valid for any unheated and heated tissue with no phase change. Note that Equation 1.5 represents two equations; one for solid tissue and another for blood.

$$\langle(\rho c_P)_i\rangle^i \frac{\partial \langle T_i\rangle^i}{\partial t} = \frac{1}{V_i}\int_{S_{out-i}} \left[(-k_i \nabla T_i) - (\rho c_P)_i u_i T_i\right].n_{out-i}\, dS + \frac{1}{V_i}\int_{S_{j-i}} (-k_i \nabla T_i).n_{j-i}\, dS + \langle Q_i\rangle^i \tag{1.5}$$

where, $i = j = T, Bl$ and $i \neq j$ and

$$\langle(\rho c_P)_i\rangle^i \frac{\partial \langle T_i\rangle^i}{\partial t} \equiv \frac{1}{V_i}\int_{V_i} (\rho c_P)_i \frac{\partial T_i}{\partial t} dV \tag{1.6}$$

1.2.2 Simplifications

The following three simplifications are made to obtain a differential form of the two-compartment GBHTM.

$$\frac{1}{V_i}\int_{S_{out-i}} (-k_i \nabla T_i) \,.\, n_{out-i}\, dS \;\equiv\; C_{i1} \nabla \,.\, k_i \nabla \langle T_i \rangle^i \tag{1.7}$$

$$\frac{1}{V_i}\int_{S_{j-i}} (-k_i \nabla T_i) \,.\, n_{j-i}\, dS \;\equiv\; \frac{(US)_{j-i}}{V_i}(\langle T_j \rangle^j - \langle T_i \rangle^i) \tag{1.8}$$

where, $i = j = T$, Bl and $i \neq j$, and

$$\frac{1}{V_i}\int_{S_{out-i}} \left[-(\rho c_p u T)_i \,.\, n_{out-i}\, dS\right] \;\equiv\; \nabla \,.\, (P c_P \langle T_i \rangle^i),\; i = Bl \tag{1.9}$$

The first simplification (Equation 1.7) relates the energy exchange among the tissue (or blood) sub-volume of an averaging volume and tissue (or blood) sub-volumes of surrounding averaging volumes to the average temperatures of tissue (or blood) sub-volumes. This simplification is similar to the simplifications used by many other BHTMs [e.g., [6–16]]. A new, to be determined, parameter C_{i1} is introduced in Equation 1.7 to keep the simplification general.

The second simplification (Equation 1.8) defines the thermal interaction between a tissue and the embedded vasculature using the tissue and blood sub-volume averaged temperatures and a heat transfer coefficient (i.e., U). Note that this heat transfer coefficient is different from conventional heat transfer coefficients and must be evaluated to appropriately implement the GBHTM since the new heat transfer coefficient is defined based on the volume-averaged temperatures. Conventional heat transfer coefficients are defined using a tissue boundary temperature and a mixed mean blood temperature.

The third simplification (Equation 1.9) is similar to the simplification proposed by Equation 1.7 and defines a new, to be determined, perfusion-related parameter P. The simplification relates the energy transported through blood vessels of a blood sub-volume to surrounding blood sub-volumes to the gradient of blood sub-volume averaged temperature.

With the above simplifications substituted in Equation 1.5, the following differential form of the two-compartment GBHTM is obtained. Equations 1.10 and 1.11 are coupled equations. Equation 1.10 is valid for the tissue sub-volume, and Equation 1.11 is valid for the blood sub-volume in an averaging volume.

$$\langle (\rho c_P)_T \rangle^T \frac{\partial \langle T_T \rangle^T}{\partial t} = C_{T1} \nabla \,.\, k_T \nabla \langle T_T \rangle^T + \frac{(US)_{Bl-T}}{V(1-\varepsilon)}(\langle T_{Bl} \rangle^{Bl} - \langle T_T \rangle^T) + \langle Q_T \rangle^T \tag{1.10}$$

$$\begin{aligned}\langle (\rho c_P)_{Bl} \rangle^{Bl} \frac{\partial \langle T_{Bl} \rangle^{Bl}}{\partial t} &= C_{Bl1} \nabla \,.\, k_{Bl} \nabla \langle T_{Bl} \rangle^{Bl} + \nabla \,.\, (P c_P \langle T_{Bl} \rangle^{Bl}) \\ &+ \frac{(US)_{Bl-T}}{V\varepsilon}(\langle T_T \rangle^T - \langle T_{Bl} \rangle^{Bl}) + \langle Q_{Bl} \rangle^{Bl}\end{aligned} \tag{1.11}$$

where, $V = V_T + V_{Bl}$ and $\varepsilon = \frac{V_{Bl}}{V}$

Note that in the above equations the local perfusion-related parameter P and the blood volume ratio ε are unknown. These values need to be determined for a given

application and tissue using imaging methods (e.g., MRI, positron emission tomography, ultrasound, etc.). Alternatively, these values can be estimated by developing physiologically realistic geometric vascular network maps and assuming mean blood flow of ~10 (diameter of vessel) m/s [17]. The tissue sub-volume V_T can be estimated as the difference between the imaging voxel volume and blood sub-volume.

1.2.3 A Three-Compartment and '*N* + 1' Compartment GBHTM

We derived above a two-compartment GBHTM by assuming that the averaging volume is composed of only two sub-volumes or compartments: a non-moving tissue sub-volume and a moving blood sub-volume. To derive a three-compartment GBHTM, let's assume, as an example, that the averaging volume is composed of the following three sub-volumes or compartments (instead of two): a non-moving tissue sub-volume, an arterial blood sub-volume, and a venous blood sub-volume. In this case, one can derive the following set of equations for a new three-compartment GBHTM using the methodology presented above and simplifications similar to the ones presented in Equations 1.7–1.9.

$$\langle(\rho c_P)_T\rangle^T \frac{\partial\langle T_T\rangle^T}{\partial t} = C_{T1}\nabla.k_T\nabla\langle T_T\rangle^T + \frac{(US)_{Ar-T}}{V(1-\varepsilon_{Ar}-\varepsilon_{Vn})}(\langle T_{Ar}\rangle^{Ar} - \langle T_T\rangle^T) + \frac{(US)_{Vn-T}}{V(1-\varepsilon_{Ar}-\varepsilon_{Vn})}(\langle T_{Vn}\rangle^{Vn} - \langle T_T\rangle^T) + \langle Q_T\rangle^T \tag{1.12}$$

$$\langle(\rho c_P)_{Ar}\rangle^{Ar} \frac{\partial\langle T_{Ar}\rangle^{Ar}}{\partial t} = C_{Ar1}\nabla.k_{Ar}\nabla\langle T_{Ar}\rangle^{Ar} + \nabla.((Pc_P)_{Ar}\langle T_{Ar}\rangle^{Ar}) + \frac{(US)_{Ar-T}}{V\varepsilon_{Ar}}(\langle T_T\rangle^T - \langle T_{Ar}\rangle^{Ar}) + \frac{(US)_{Ar-Vn}}{V\varepsilon_{Ar}}(\langle T_{Vn}\rangle^{Vn} - \langle T_{Ar}\rangle^{Ar}) + \langle Q_{Ar}\rangle^{Ar} \tag{1.13}$$

$$\langle(\rho c_P)_{Vn}\rangle^{Vn} \frac{\partial\langle T_{Vn}\rangle^{Vn}}{\partial t} = C_{Vn1}\nabla.k_{Vn}\nabla\langle T_{Vn}\rangle^{Vn} + \nabla.((Pc_P)_{Vn}\langle T_{Vn}\rangle^{Vn}) + \frac{(US)_{Vn-T}}{V\varepsilon_{Vn}}(\langle T_T\rangle^T - \langle T_{Vn}\rangle^{Vn}) + \frac{(US)_{Ar-Vn}}{V\varepsilon_{Vn}}(\langle T_{Ar}\rangle^{Ar} - \langle T_{Vn}\rangle^{Vn}) + \langle Q_{Vn}\rangle^{Vn} \tag{1.14}$$

where, $V = V_T + V_{ar} + V_{vn}$, $\varepsilon_{Ar} = \frac{V_{Ar}}{V}$ and $\varepsilon_{Vn} = \frac{V_{Vn}}{V}$. A point to note in this new GBHTM is that it is relatively more complex than the two-compartment GBHTM presented in Equations 1.10 and 1.11. In this new, three-compartment GBHTM, we have created a need to separately identify and account for the two blood sub-volumes (i.e., arterial and venous blood in this example) to solve for *in vivo* temperatures, which may or may not be useful and/or feasible for a given application. Also, the sub-volumes don't have to be arterial or venous sub-volumes. One can think about creating blood sub-volumes based on the relative thermal importance and frequency of blood vessels, as well. Generalizing the above result further, the following set of equations can be obtained for a GBHTM where the averaging volume is composed of '$N + 1$' compartments: a non-moving tissue

sub-volume and 'N' blood sub-volumes.

$$\langle(\rho c_P)_T\rangle^T \frac{\partial\langle T_T\rangle^T}{\partial t} = C_{T1}\nabla.k_T\nabla\langle T_T\rangle^T + \sum_{i=1}^{N}\frac{(US)_{i-T}}{V\left(1-\sum_{j=1}^{N}\varepsilon_j\right)}(\langle T_i\rangle^i - \langle T_T\rangle^T) + \langle Q_T\rangle^T \tag{1.15}$$

$$\langle(\rho c_P)_i\rangle^i \frac{\partial\langle T_i\rangle^i}{\partial t} = C_{i1}\nabla.k_i\nabla\langle T_i\rangle^i + \nabla.((Pc_P)_i\langle T_i\rangle^i) + \frac{(US)_{i-T}}{V\varepsilon_i}(\langle T_T\rangle^T - \langle T_i\rangle^i) + \sum_{j=1}^{N}\frac{(US)_{i-j}}{V\varepsilon_i}(\langle T_j\rangle^j - \langle T_i\rangle^i) + \langle Q_i\rangle^i \tag{1.16}$$

where, $i, j = 1\ldots N$ blood sub-volumes, $i \neq j$, $V = V_T + \sum_{i=1}^{N} V_i$ and $\varepsilon_i = \frac{V_i}{V}$.

1.3 Comparing the Two-Compartment GBHTM with Pennes' BHTM

Pennes' BHTM is a simple and widely used BHTM [6] that was intuitively proposed by a clinician named Henry H. Pennes in 1948 to predict *in vivo* temperatures (Equation 1.17).

$$(\rho c_P)_T\frac{\partial T_T}{\partial t} = \nabla.k_T\nabla T_T + w(c_P)_{Bl}(1-\zeta)(T_{Bl} - T_T) + Q_T \tag{1.17}$$

Traditionally, Pennes' BHTM has been a point of contention and a source of confusion. This is so because the lack of a formal derivation of Pennes' BHTM makes it difficult to interpret Pennes' variables, parameters, and results in terms of the underlying physiology. For example, it is not clear what 'blood temperature' is in the Pennes' model. Thermodynamically, the blood temperature in Pennes' BHTM can be defined in at least four different ways: (1) local, point-wise true blood temperature, (2) blood velocity-weighted blood vessel area-averaged blood temperature, (3) blood vessel area-averaged blood temperature and (4) perfused tissue volume-averaged blood temperature. Assuming the blood temperature as the point-wise true temperature or the velocity-weighted temperature makes Pennes' BHTM physically invalid since it makes the model violate first principles. Assuming the blood temperature as the area-averaged or volume-averaged temperature renders physically invalid the traditional conception of the Pennes' w term as a blood flow term. It should be noted, however, that Pennes' BHTM has been shown to be capable of predicting reasonably accurate *in vivo* temperatures in 'local' tissue regions for 'short' durations by adjusting Pennes' perfusion-related parameter $w(c_p)_{Bl}(1-\zeta)$ to minimize error between model predictions and measurements. Adjusting Pennes' perfusion related parameter $w(c_p)_{Bl}(1-\zeta)$ is necessary because of the lack of a formal derivation of Pennes' BHTM, which makes it difficult to evaluate the parameter independently based on the underlying physiology. Simplicity and reasonable performance of Pennes' BHTM (once the blood-perfusion-related parameter $w(c_p)_{Bl}(1-\zeta)$ is adjusted, of course) has always been puzzling for a 'physically and theoretically invalid' model.

Let's compare Pennes' BHTM with the two-compartment GBHTM to gain a better understanding of the implicit and explicit assumptions, and thus the application regimes of Pennes' model. Comparing Pennes' BHTM with the newly developed two-compartment GBHTM one notes the following:

1. The basic form of Equation 1.17 (i.e., Pennes' BHTM) and Equation 1.10 (i.e., the tissue sub-volume equation in the GBHTM) is similar (with $C_{T1} = 1$). Thus, Pennes' tissue temperature and blood temperature should be interpreted as a volume-averaged tissue temperature and a volume-averaged blood temperature, respectively, instead of the point-wise true temperatures. Tissue properties (e.g., density, specific heat, conductivity) and source term should also be interpreted as volume-averaged quantities.
2. Pennes' blood perfusion related parameter $w(c_p)_{Bl}(1-\zeta)$ should be interpreted as equivalent to the blood-tissue heat transfer rate term$(US)_{T\text{-}Bl}/V\,(1\text{-}\varepsilon)$ in the GBHTM. In practice, Pennes' blood perfusion related parameter $w(c_p)_{Bl}(1-\zeta)$ is always determined by minimizing the error between the modeled and measured temperatures to obtain reasonable estimates of the in vivo temperatures. This is equivalent to obtaining $(US)_{T\text{-}Bl}/V\,(1\text{-}\varepsilon)$ values by minimizing the error.
3. Pennes' BHTM assumes the blood temperature as constant. This is equivalent to assuming that the blood has infinite thermal capacity in the two-compartment GBHTM. Thus, Pennes' BHTM artificially forces tissue temperatures to stay close to the assumed blood temperature. The assumption results in the overestimation of the blood-tissue heat transfer rate and the underestimation of the tissue heating in deep tissues due to source terms. The lack of the ability to model the blood temperature variation further limits Pennes' BHTM to applications where the blood temperature does not vary 'significantly' from the assumed value in space and time.
4. Pennes introduced a blood equilibration parameter ζ $(0 \le \zeta \le 1)$ to quantify the blood-tissue heat transfer rate based on the local blood flow w. However, the spatial and temporal behavior of this parameter ζ is never studied in vivo. In the absence of a known spatial and temporal variation of ζ for an application and tissue type, substituting local blood flow value for w in Pennes' model estimates blood-tissue heat transfer rate incorrectly. Substituting local blood perfusion values for the term w (assuming $\zeta = 0$) or $w(1\text{-}\zeta)$ (assuming $\zeta \neq 0$) and the absence of an equation for modeling the blood sub-volume averaged blood temperature variation in Pennes' BHTM have been shown to result in large deviations between the predictions of the model and the absolute temperature field in vascularized tissues [18].

1.4 Comparing the Predictions of the Two-Compartment GBHTM and Pennes' BHTM with Measured *in vivo* Temperature Changes during MRI

Figures 1.1–1.4, below compare the predictions of the two-compartment GBHTM and Pennes' BHTM with the temperature changes measured in swine during MRI. MRI scanners deposit radio frequency (RF) energy inside the body during MRI,

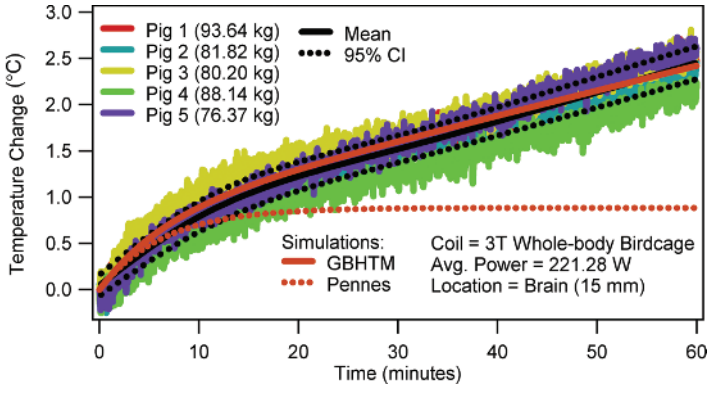

Figure 1.1 RF power deposition-induced brain heating, as measured with a fluoroptic probe placed 15 mm deep in the swine brain after the dura, in a 3T (Larmor frequency = ~123.2 MHz) MRI scanner. The RF power was delivered using a body coil with the swine head placed in the isocenter.

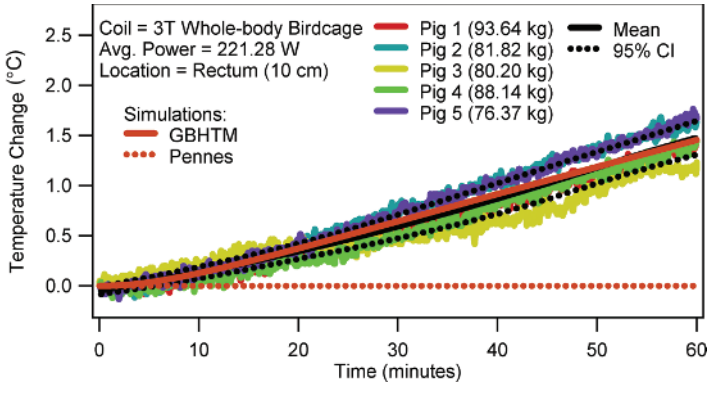

Figure 1.2 RF power deposition-induced whole-body heating, as measured with a fluoroptic probe placed 10 cm deep in the swine rectum, in a 3T (Larmor frequency = ~123.2 MHz) MRI scanner. The RF power was delivered using a body coil with the swine head placed in the isocenter.

which produces heating. Accurate prediction of this heating is necessary for the safety and efficacy of the scanners. Note that Pennes' BHTM is implemented by assuming infinite thermal capacity of the blood in the two-compartment GBHTM, as it should.

As discussed above, the figures clearly demonstrate that (1) the two-compartment GBHTM predicts *in vivo* tissue heating accurately in space and time, (2) appropriately implemented Pennes' BHTM predicts tissue heating accurately only until the blood temperature does not start varying appreciably in space and time from the baseline value, and (3) the assumption of constant blood temperature makes Pennes' BHTM overestimate the blood-tissue heat transfer rate, and thus underestimate the deep tissue heating. More details regarding the experimental evaluation of the two-compartment GBHTM and Pennes' BHTM can be found in [19, 20].

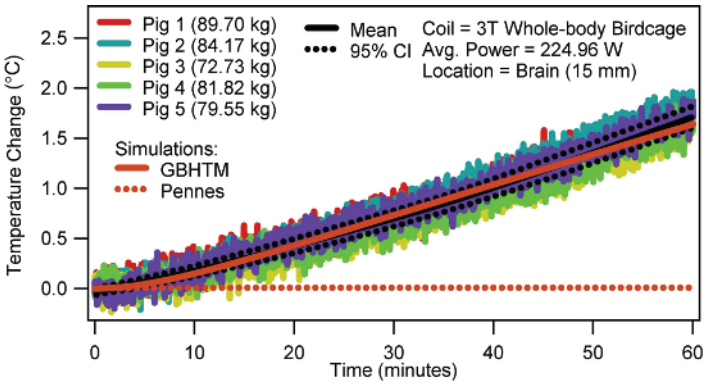

Figure 1.3 RF power deposition-induced brain heating, as measured with a fluoroptic probe placed 15 mm deep in the swine brain after the dura, in a 3T (Larmor frequency = ~123.2 MHz) MRI scanner. The RF power was delivered using a body coil with the center of the swine trunk placed in the isocenter.

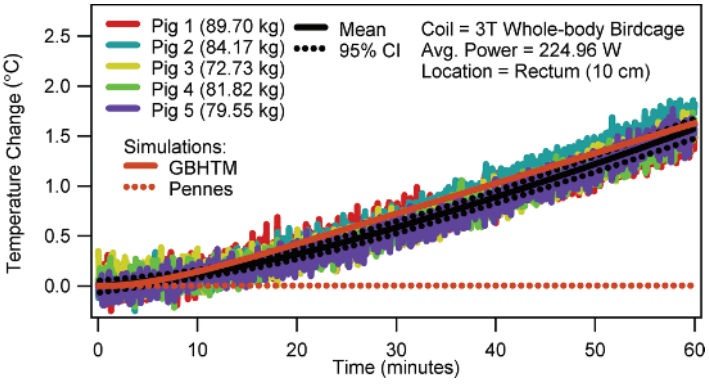

Figure 1.4 RF power deposition-induced whole-body heating, as measured with a fluoroptic probe placed 10 cm deep in the swine rectum, in a 3T (Larmor frequency = ~123.2 MHz) MRI scanner. The RF power was delivered using a body coil with the center of the swine trunk placed in the isocenter.

1.5 Summary

A general methodology is presented to derive BHTMs from first principles. The methodology was used to, first, derive a general 'two-compartment' BHTM for perfused tissues with very few assumptions – herein called the two-compartment generic bioheat transfer model (GBHTM). Later, the same methodology was used to derive more general forms of the model (i.e., a three-compartment GBHTM and an '$N + 1$' compartment GBHTM). Finally, the new, two-compartment GBHTM was compared with the empirical, 'gold standard' Pennes' BHTM, theoretically as well as experimentally, to better understand the potential and limitations of the GBHTM and Pennes' BHTM. The comparison helped better understand the relation between the variables and parameters of Pennes' BHTM and the underlying physiology. It was demonstrated that the two-compartment GBHTM predicted accurate *in vivo*

tissue heating in space and time while an appropriately implemented Pennes' BHTM predicted accurate *in vivo* tissue heating when the blood temperature did not change 'appreciably' from the baseline value.

Disclaimer

The subject matter, content, and views presented do not represent the views of the Department of Health and Human Services (HHS), US Food and Drug Administration (FDA), and/or the United States.

Nomenclature

c_p	specific heat (J/(kg·K))
D	vessel diameter (m)
k	thermal conductivity (W/(m·K))
n_{i-j}	normal vector from i to j
P	Perfusion vector (kg/(m^2·s))
Q	power (W/m^3)
S_{i-j}	surface area between volume i and j (m^2)
T	temperature (K)
U	heat transfer coefficient
t	time (s)
u	velocity (m/s)
V	volume (m^3)
w	Pennes' perfusion-related term

Subscripts

Ar	arterial
Bl	blood
T	tissue
Vn	venous

Greek

β	blood volume over imaged voxel volume
ε	blood volume fraction
ζ	Pennes' equilibration term (0–1)
ρ	density (kg/m^3)

References

1 Kays, W. M. & Crawford, M. E., 1993, *Convective Heat and Mass Transfer*, New York, McGraw-Hill, Inc.

2 White, J. A., Dutton, A. W., Schmidt, J. A., and Roemer, R. B., 2000, An accurate, convective energy equation based automated meshing technique for analysis of blood vessels and tissues, *Int. J. Hyperthermia*, 16(2): 145–158.

3 Roemer, R. B., 1999, Engineering aspects of hyperthermia therapy, *Annu Rev Biomed Eng*, 1: 347–376.

4 Craciunescu, O. I., Raaymakers, B. W., Kotte, A. N., et al., 2001, Discretizing large traceable vessels and using DE-MRI perfusion maps yields numerical temperature contours that match the MR noninvasive measurements, *Med Phys*, 28: 2289–2296.

5 Shrivastava, D. and Vaughan, J. T., 2009, A generic bioheat transfer thermal model for a perfused tissue, *ASME: Journal of Biomechanical Engineering*, 131(7): 074506.

6 Pennes, H. H., 1998, Analysis of tissue and arterial blood temperatures in the resting human forearm: 1948, *J Appl Physiol*, 85: 5–34.

7 Wulff, W., 1974, The energy conservation equation for living tissue, *IEEE Trans Biomed Eng*, BME-21: 494–495.

8 Klinger, H. G., 1974, Heat transfer in perfused biological tissue: I: General theory, *Bull Math Biol*, 36: 403–415.

9 Klinger, H. G., 1978, Heat transfer in perfused biological tissue: II: The macroscopic temperature distribution in tissue, *Bull Math Biol*, 40: 183–199.

10 Chen, M. M. and Holmes, K. R., 1980, Microvascular contributions in tissue heat transfer, *Ann N Y Acad Sci*, 335: 137–150.

11 Osman, M. M. and Afify, E. M., 1984, Thermal modeling of the normal woman's breast, *J Biomech Eng*, 106: 123–130.

12 Weinbaum, S. and Jiji, L. M., 1985, A new simplified bioheat equation for the effect of blood flow on local average tissue temperature, *J Biomech Eng*, 107: 131–139.

13 Brinck, H. and Werner, J., 1994, Efficiency function: Improvement of classical bioheat approach, *J Appl Physiol*, 77: 1617–1622.

14 Weinbaum, S., Xu, L. X., Zhu, L., and Ekpene, A., 1997, A new fundamental bioheat equation for muscle tissue: Part I: Blood perfusion term, *J Biomech Eng*, 119: 278–288.

15 Roemer, R. B. and Dutton, A. W., 1998, A generic tissue convective energy balance equation: Part I: Theory and derivation, *J Biomech Eng*, 120: 395–404.

16 Wren, J., Karlsson, M., and Loyd, D., 2001, A hybrid equation for simulation of perfused tissue during thermal treatment, *Int J Hyperthermia*, 17: 483–498.

17 Chato, J. C., 1980, Heat transfer to blood vessels, *J Biomech Eng*, 102: 110–118.

18 Brinck, H. and Werner, J., 1995, Use of vascular and non-vascular models for the assessment of temperature distribution during induced hyperthermia, *Int J Hyperthermia*, 11: 615–626.

19 Shrivastava, D., Utecht, L., Tian, J., et al. 2014, *In vivo* radiofrequency heating in swine in a 3T (123.2 MHz) birdcage whole-body coil, *Magnetic Resonance in Medicine*, 72(4): 1141–50.

20 Shrivastava, D., Hanson, T., Kulesa, J., et al., 2011, Radiofrequency heating in porcine models with a 'large' 32 cm internal diameter, 7 T (296 MHz) head coil, *Magnetic Resonance in Medicine*, 66(1): 255–263.